Skyrmion lattices in metallic and semiconducting B20 transition metal compounds

2010 J. Phys.: Condens. Matter 22 164207

(http://iopscience.iop.org/0953-8984/22/16/164207)

J. Phys.: Condens. Matter **22** (2010) 164207 (7pp) doi:10.1088/0953-8984/22/16/164207

Skyrmion lattices in metallic and semiconducting B20 transition metal compounds

C Pfleiderer[1], T Adams[1], A Bauer[1], W Biberacher[2], B Binz[3], F Birkelbach[1], P Böni[1], C Franz[1], R Georgii[1,4], M Janoschek[1], F Jonietz[1], T Keller[5], R Ritz[1], S Mühlbauer[1], W Münzer[1], A Neubauer[1], B Pedersen[1] and A Rosch[3]

[1] Physik Department E21, TU München, D-85748 Garching, Germany
[2] BADW München, Walther Meissner Institute, D-85748 Garching, Germany
[3] ITP, University of Cologne, D-50937 Cologne, Germany
[4] Forschungsneutronenquelle Heinz-Maier-Leibnitz FRM II, TU München, D-85748 Garching, Germany
[5] MPI für Festkörperforschung, Heisenbergstraße 1, D-70569 Stuttgart, Germany

E-mail: christian.pfleiderer@frm2.tum.de

Received 1 September 2009
Published 30 March 2010
Online at stacks.iop.org/JPhysCM/22/164207

Abstract
High pressure studies in MnSi suggest the existence of a non-Fermi liquid state without quantum criticality. The observation of partial magnetic order in a small pocket of the pressure versus temperature phase diagram of MnSi has additionally inspired several proposals of complex spin textures in chiral magnets. We used neutron scattering to observe the formation of a two-dimensional lattice of skyrmion lines, a type of magnetic vortices, under applied magnetic fields in metallic and semiconducting B20 compounds. In strongly disordered systems the skyrmion lattice is hysteretic and extends over a large temperature range. Our study experimentally establishes magnetic materials lacking inversion symmetry as an arena for new forms of spin order composed of topologically stable spin textures.

(Some figures in this article are in colour only in the electronic version)

1. Introduction

The properties of the transition metal system MnSi generate great interest in the areas of itinerant-electron magnetism and complex spin order. MnSi orders helimagnetically below a transition temperature $T_c = 29.5$ K, where the helical modulation, $\lambda_h \approx 190$ Å, is large in comparison to the lattice constant ($a = 4.58$ Å). Hence on length scales of a few lattice constants the magnetic properties are essentially those of a ferromagnet. Likewise across the entire Brillouin zone a strongly exchange-enhanced spectrum of ferromagnetic spin fluctuations is observed [1]. In fact, measurements of the spin fluctuations in MnSi in the early 1980s allowed one, for the first time, to establish the quantitative agreement of spin fluctuation theory with experiment [2, 3].

In a parallel development polarized neutron scattering studies in the early 1980s identified the helimagnetism in MnSi as the first example of a homochiral spin spiral [6] as first predicted by Dzyaloshinsky in the late 1950s. The weak Dzyaloshinsky–Moriya interactions thereby originate in the lack of inversion symmetry of the B20 crystal structure and the direction of the helical modulation is pinned to the cubic space diagonals of the crystal structure by weak crystal field interactions (higher-order spin–orbit coupling). This makes MnSi an example *par excellence* for a material with a well-defined hierarchy of energy scales. Recent inelastic neutron scattering studies in MnSi underscore this observation, which established the formation of intense helimagnon bands of universal character [7].

Based on the excellent quantitative agreement of spin fluctuation theory with weakly ferromagnetic itinerant-electron

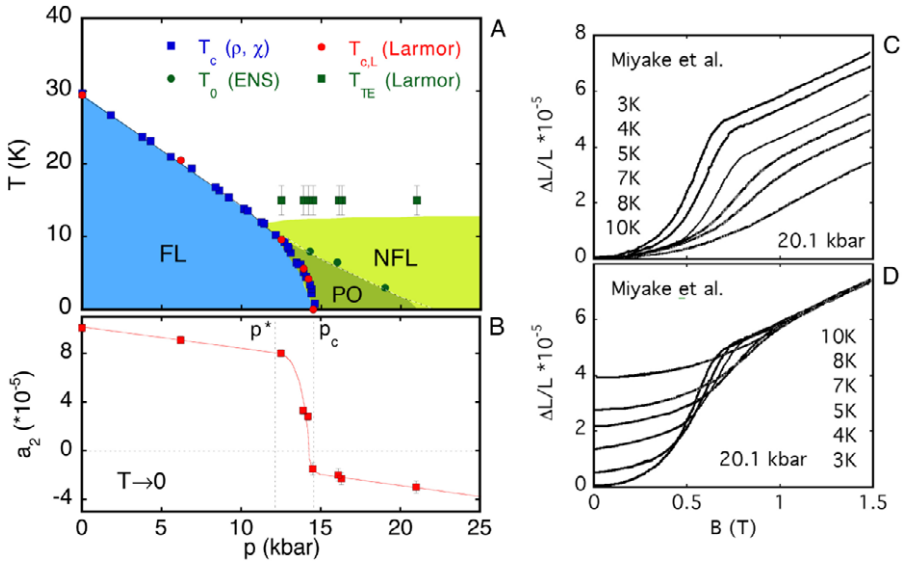

Figure 1. (A) Pressure versus temperature phase diagram of MnSi, as shown in references [19, 20] and reported in [4]. (B) Magnetic contribution to the lattice constant, a_2, inferred from Larmor diffraction [4] by subtracting a lattice contribution due to phonons as extrapolated from temperatures above ∼15 K. Above the critical pressure a weakly pressure-dependent negative value of a_2 is observed. (C) Relative change of lattice constant as a function of magnetic field at 20.1 kbar inferred from strain gauge measurements as reported in [5]. (D) Data reported in [5], but now shifted to match at high fields. This presentation underscores the presence of the spontaneous lattice contraction below ∼10 K for zero field, in remarkable quantitative agreement with the Larmor data.

systems a detailed search for ferromagnetic quantum criticality began in the late 1980s, focusing at first on MnSi [8, 9]. The aim of these studies was twofold: first, to establish the possible existence of marginal Fermi liquid behavior and, second, to search for superconductivity at the border of magnetism later discovered in certain f-electron systems [10].

The temperature versus pressure phase diagram of MnSi is shown in figure 1(A). With increasing pressure the transition temperature T_c as inferred from the resistivity ρ and AC susceptibility χ decreases and vanishes for $p_c = 14.6$ kbar [11]. For low pressures the resistivity follows the quadratic temperature dependence of a weakly spin-polarized Fermi liquid (FL). However, at p_c the resistivity abruptly changes to a $T^{3/2}$ non-Fermi liquid (NFL) dependence [12–14]. This NFL resistivity extends over an exceptionally wide range in temperature, pressure and magnetic field [15]. The NFL resistivity is surprising in particular, because above a pressure $p^* \approx 12$ kbar the AC susceptibility displays a discontinuous (first-order) transition at T_c and itinerant metamagnetism. In fact, very weak first-order characteristics of the helimagnetic transition may even be seen at ambient pressure [16], as underscored by recent susceptibility studies [17] (unfortunately no field dependence is reported in [17]).

To identify the origin of the NFL behavior the pressure dependence of the helimagnetic order was studied by neutron scattering [18]. In contrast to expectation, the ordered magnetic moment does not track T_c to zero for $p \to p_c$. Instead it seems to survive above p_c in a small temperature versus pressure regime. Moreover, the scattering intensity was found to be spread over the surface of a small sphere in reciprocal space with unusual intensity maxima for the ⟨110⟩ directions. Being reminiscent of structure factors in liquid crystals, the peculiar magnetic scattering intensity is referred to as partial magnetic order (PO).

The first-order behavior as a function of pressure is supported by the temperature dependence of the partial magnetic order and the helimagnetic order, which early on suggested some form of electronic phase segregation. Further microscopic evidence for such a phase segregation may be inferred from muon spin rotation in the form of a decreasing volume fraction of helical order above $p^* \approx 12$ kbar [21]. These studies suggest that the partial order is dynamic. The pressure and temperature dependence of the lattice constant as measured by neutron Larmor diffraction, finally, provided strong evidence that the NFL resistivity emerges without quantum criticality [4].

A key feature revealed by the Larmor diffraction study is a spontaneous volume contraction, a_2, with respect to the quadratic temperature dependence of the lattice constant observed at high temperatures (figure 1(B)). The existence of this contraction is strongly supported by a recent study using a strain gauge [5]. Unfortunately this study does not report the temperature dependence over a sufficiently large range (probably due to the technical limitations of this method). The magnetic field dependence as published for 20.1 kbar is shown in figure 1(C). As shown in figure 1(D) these data reveal an additional contraction for low fields, in remarkable quantitative agreement with a_2, when plotting $\Delta L/L$ with respect to the magnetic field dependence at high fields at 10 K. Thus the lattice contraction exists essentially over the regime of the NFL resistivity, representing a key thermodynamic feature.

Taken together the high pressure studies provide evidence of the formation of a highly unusual metallic state. The partial magnetic order, believed to be an important microscopic signature, has inspired various theoretical proposals of

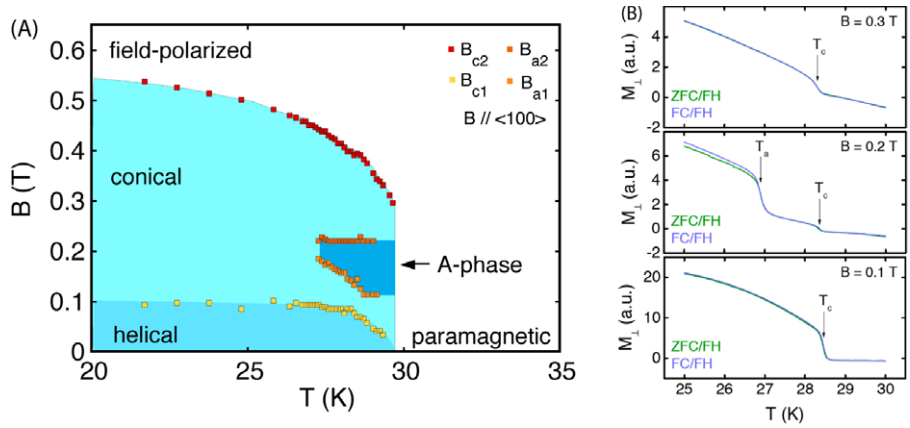

Figure 2. (A) Magnetic phase diagram of MnSi, where the phase boundaries have been inferred from the AC susceptibility. The spin structure of the A-phase was recently identified as the first example of a skyrmion lattice in a chiral magnet [19, 20]. (B) Torque magnetization as a function of temperature. In the A-phase the torque is minimal, as expected for a spin structure along an easy magnetic axis. The abrupt changes at the border of the A-phase suggest a clear phase transition.

unconventional spin textures with non-trivial topology in cubic materials involving various fairly strong assumptions [22–26]. In fact, a long time ago Bogdanov and collaborators were the first to predict the formation of skyrmion lattices in anisotropic chiral magnets using a mean-field model [27, 28].

Based on a study of the effects of spin transfer torques in MnSi to be reported elsewhere, we have recently noticed [19] that the A-phase in the magnetic phase diagram of MnSi (figure 2(A)) in fact represents such a long sought skyrmion lattice in a chiral magnet (for early experimental work on the A-phase see [29–31]). The key signature of the skyrmion lattice in MnSi in neutron scattering for a field parallel to the incident neutron beam is an intensity pattern with a sixfold symmetry—regardless of the direction of the applied magnetic field with respect to the crystallographic orientation. Thus the skyrmion lattice decouples very efficiently from the crystal lattice. Because the skyrmion lattice represents a new form of magnetic order, we have explored the possible existence of skyrmion lattices in other B20 compounds, notably for the series $Mn_{1-x}Fe_xSi$, $Mn_{1-x}Co_xSi$ and $Fe_{1-x}Co_xSi$. As our main conclusions the skyrmion lattice forms, regardless of whether the host material is a pure metal or a weakly doped metal, or even a strongly disordered semiconductor.

2. Experimental techniques

Single crystals of MnSi, $Mn_{1-x}Fe_xSi$, $Mn_{1-x}Co_xSi$ and $Fe_{1-x}Co_xSi$, were grown by optical float-zoning using an ultra-high-vacuum (UHV)-compatible image furnace under a purified Ar atmosphere. The float-zoned ingots were first characterized by means of a light microscope after polishing one side, where large single-grain sections were observed. The single-crystal character was confirmed using Laue x-ray diffraction on several sides of the ingot. Excellent single crystallinity was established for some of the crystals studied on the four-circle neutron diffractometer RESI at FRM II.

Comprehensive measurements of the magnetization, AC susceptibility and specific heat were carried out for all systems with a Quantum Design Physical Properties Measurement System for temperatures down to 2 K and magnetic fields up to 9 T. The magneto-transport properties were measured down to 1.5 K at magnetic fields up to 14 T with a standard He system (the transport data will not be discussed in this paper). All of the data measured established the excellent quality of all of our samples. First studies of the torque magnetization across the magnetic phase diagram of MnSi were carried out with a capacitive torque meter [32]. While the phase transitions and general features of the torque magnetization could be determined very well, our field-dependent data were subject to a small hysteretic background of unknown origin.

Our small-angle neutron scattering measurements were carried out at the cold diffractometer MIRA at FRM II. Data were typically recorded for neutrons with a wavelength $\lambda = 9.7$ Å $\pm$ 5%. Backgrounds were determined at high temperatures and subtracted accordingly. For the SANS measurements the samples were cooled with a pulse-tube cooler. Magnetic fields were applied with a bespoke pair of water-cooled Helmholtz coils [33].

3. Results

The torque magnetization of MnSi, for a $\langle 100 \rangle$ axis shown in figure 2(B), underscores the peculiar nature of the skyrmion lattice in MnSi (see also [34]). The data shown here have not been corrected for small contributions due to the thermal expansion and magnetostriction of the empty torque meter. As a function of temperature the helimagnetic transition is accompanied by a pronounced change of slope at T_c. The data for $B = 0.2$ T additionally exhibits a plateau in the regime of the A-phase. Likewise, as a function of magnetic field (data not shown) the torque magnetization displays a large, strongly field-dependent contribution. However, in the regime of the A-phase the torque magnetization drops abruptly to a low value. This is consistent with an easy magnetic axis and the observation in neutron scattering, that the skyrmion lattice always forms perpendicular to the applied magnetic field regardless of the field direction with respect to the crystal lattice. Further, the torque data clearly shows a phase transition at the border of the A-phase, characteristic of weak first-order

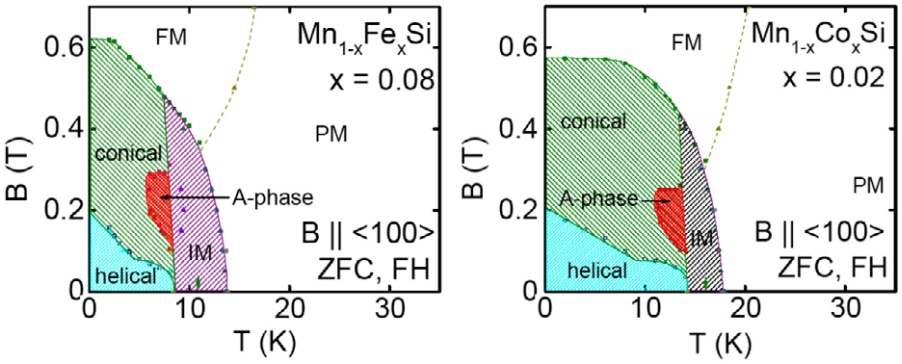

Figure 3. Magnetic phase diagrams of $Mn_{1-x}Fe_xSi$ for $x = 8\%$ and $Mn_{1-x}Co_xSi$ for $x = 2\%$. The phase boundaries were inferred from measurements of the magnetization, AC susceptibility and specific heat. The following abbreviations are used: paramagnetism (PM), ferromagnetism (FM), intermediate phase (IM), zero-field-cooled (ZFC) and field-heated (FH).

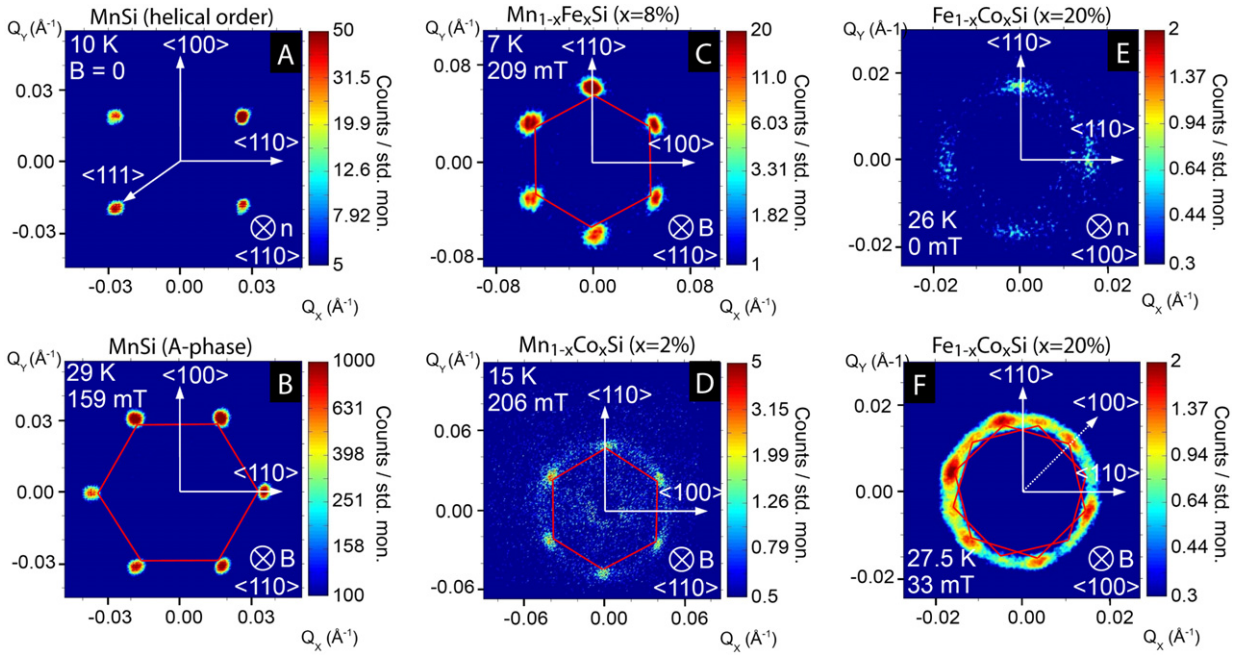

Figure 4. Typical intensity distributions recorded in small-angle neutron scattering of the helical order and A-phase in MnSi, $Mn_{1-x}Fe_xSi$, $Mn_{1-x}Co_xSi$ and $Fe_{1-x}Co_xSi$. Note the different scales and accordingly the differences of ordering wavelength between the different systems. At the same time also note that there are no differences in the wavelength of the magnetic modulation between zero-field helical order and skyrmion lattice in the A-phase.

transitions both as a function of temperature and magnetic field.

Several studies have addressed the evolution of the magnetic phase diagram of MnSi, when substitutionally replacing Mn by Fe and Co. In our study we find that the magnetization, susceptibility and specific heat are perfectly consistent with previous work [35–37]. A detailed account of our work [38, 39] will be published elsewhere. As shown in figure 3 doping with Fe and Co substantially reduces the magnetic transition temperature. Similar to MnSi it is possible to distinguish six regimes in the phase diagram of both $Mn_{1-x}Fe_xSi$ and $Mn_{1-x}Co_xSi$. Taking into account our small-angle neutron scattering data, these regimes are: (i) paramagnetism with a strong Curie–Weiss susceptibility at high temperatures and low fields, (ii) helimagnetic order at zero magnetic field and low temperatures, (iii) conical order at low magnetic fields and low temperatures, (iv) the A-phase in low fields closely below the helimagnetic ordering temperature, (v) an intermediate regime that has not been identified unambiguously at low fields and temperatures just above the helimagnetic transition temperature and (vi) a field-polarized ferromagnetic regime at high fields and low temperatures.

Typical neutron scattering intensity patterns in the zero-field-cooled helimagnetic state and the A-phase observed in MnSi, $Mn_{1-x}Fe_xSi$, $Mn_{1-x}Co_xSi$ and $Fe_{1-x}Co_xSi$, are summarized in figure 4. We note that the scales of the data shown here differ substantially between all compounds. In MnSi the sharp spots characteristic of the helical modulation in the ⟨111⟩ directions are observed (figure 4(A)). Note that

the spots in the helical phase are resolution-limited, while the rocking width is ∼3°. The latter is consistent with all data published, suggesting magnetic coherence lengths in excess of 10^4 Å. The scattering pattern changes dramatically in the A-phase, where a sixfold symmetry is observed for a magnetic field applied parallel to the incident neutron beam (figure 4(B)).

For $Mn_{1-x}Fe_xSi$ ($x = 8\%$) and $Mn_{1-x}Co_xSi$ ($x = 2\%$) the scattering patterns are quite similar. However, we find considerable azimuthal broadening of the intensity in the helically ordered state (not shown). In contrast, in the A-phase of $Mn_{1-x}Fe_xSi$ and $Mn_{1-x}Co_xSi$ shown in figures 4(C) and (D) the spots remain very well defined and sharp, exhibiting the sixfold symmetry observed in pure MnSi. This suggests that doping with Fe or Co reduces the pinning potential for the direction of the helical order. At the same time the unchanged sharp scattering pattern and sixfold symmetry observed in the A-phase clearly establish that the skyrmion lattice is essentially unchanged even though the electronic state is now that of a weakly disordered metal.

More detailed measurements of the magnetic field dependence suggest that there is essentially no hysteretic behavior of the scattering pattern observed in the A-phase. This contrasts with the properties of $Fe_{1-x}Co_xSi$ [40]. Already the scattering pattern in the zero-field-cooled state differs substantially from that observed in pure MnSi, as well as $Mn_{1-x}Fe_xSi$ and $Mn_{1-x}Co_xSi$. As shown in figure 4(E) the spontaneous magnetic order is characterized by very broad intensity maxima in the ⟨110⟩ direction. This was entirely unexpected since previous studies reported maxima for the ⟨100⟩ directions [41–43]. We therefore thoroughly checked and confirmed our observations in various ways (see [40] for further details). The ZFC intensity pattern of $Fe_{1-x}Co_xSi$ ($x = 20\%$) is highly reminiscent of the partial magnetic order observed in MnSi at high pressures [40].

Moreover, a typical intensity pattern recorded after field-cooling into the A-phase of $Fe_{1-x}Co_xSi$ is shown in figure 4(F). For a magnetic field applied parallel to ⟨100⟩ a total of twelve spots are observed. Of these twelve spots two sets of six spots may be distinguished, each of which is aligned with one of the two ⟨100⟩ directions in the scattering plane. A more detailed analysis of the azimuthal variation of the scattering intensity strongly suggests that the twelve spots originate from two domain populations, each with the characteristic sixfold scattering pattern of the skyrmion lattice [40, 44]. In summary, the skyrmion lattice survives even in a strongly doped semiconductor. However, here strongly hysteretic properties are observed, suggesting that the disorder interferes substantially with the mechanisms driving the formation of the skyrmion lattice.

4. Discussion

The key feature of the spin structure observed in small-angle neutron scattering in the A-phase of the B20 compounds studied is a sixfold symmetry of the scattering pattern. The scattering pattern is thereby strictly perpendicular to the direction of the applied magnetic field. We have so far not observed higher harmonic reflections in any of the compounds, suggesting that they may be very weak. However, to settle the question for higher harmonics requires the use of a state-of-the-art high intensity small-angle neutron scattering beamline. In turn, neutron scattering at the moment does not allow us to distinguish whether the spin structure represents a multi-domain single-k structure or a single-domain multi-k structure. In MnSi the unambiguous identification of the spin structure as a skyrmion lattice is instead based on very strong theoretical arguments and the observation of the so-called topological Hall effect.

The theoretical analysis is based on a mean-field model describing multi-$\vec{k}$ structures [22, 23]. Here the lowest level mode–mode coupling in the presence of the Dzyaloshinsky–Moriya interactions under an applied magnetic field favors energetically the formation of a multi-k structure with $\sum_i \vec{k}_i = 0$ and directions of $\vec{k}$ that are perpendicular to the applied field. The most beneficial situation is obtained for a triple-$\vec{k}$ state with small corrections from higher harmonics. In contrast, it is energetically extremely costly to align a single-$\vec{k}$ modulation perpendicular to an applied magnetic field. On a mean-field level the triple-$\vec{k}$ state perpendicular to the applied magnetic field is metastable in cubic systems. However, it is possible to show that Gaussian thermal fluctuations in the vicinity of the helical transition temperature stabilizes the triple-$\vec{k}$ state as the ground state thus forming a spin crystal (inset of figure 5). The resulting magnetic phase diagram shares remarkable similarities with that observed experimentally, where the model accounts for *all features* observed experimentally (figure 5; for further details see [19]). As an important aside, the variation of the magnitude of the magnetization (difference between minimum to maximum magnitude) is *smallest* in the field range of the A-phase, suggesting that the system prefers to avoid gradients of the magnetization rather than developing a softened amplitude. This is shown in figure 5(B), where the constant magnetization modulus $|M| = 1$ corresponds to the magnetization in the conical phase.

When analyzing in more detail the skyrmion density of the triple-$\vec{k}$ structure (the Gaussian fluctuations and higher harmonics do not change the topological properties of the spin structure), the integrated skyrmion density, $\Phi = -1$, corresponds to one skyrmion per magnetic unit cell, where the magnetization in the core of the skyrmion is aligned anti-parallel to the applied magnetic field. In order to establish this topological property of the spin structure experimentally, it is possible to measure the Hall effect [45]. As the conduction electrons propagate through the material, they follow the gradual variation of spin direction adiabatically, thereby collecting a Berry phase that acts like an additional effective magnetic field. This field gives rise to an additional contribution in the Hall signal, referred to as the topological Hall effect (THE). In fact, the sign and magnitude of the THE observed in MnSi is in very good quantitative agreement with experiment (studies of the other B20 systems mentioned here are underway) [20].

As a different piece of experimental evidence suggesting the formation of a skyrmion lattice our studies of $Fe_{1-x}Co_xSi$ for the field parallel ⟨100⟩ reveals twelve intensity maxima;

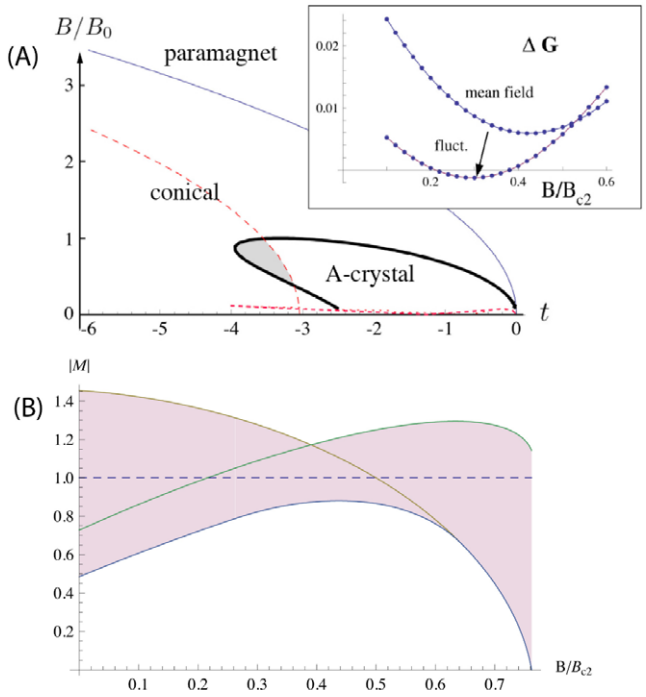

Figure 5. (A) Calculated magnetic phase diagram as a function of the distance t to the helimagnetic transition [19]. The inset displays the reduction of the minimum of the free energy in a mean-field approximation due to fluctuations. (B) Magnetic field dependence of the largest and smallest magnetization amplitudes [19]. In the field range where the skyrmion lattice becomes stable, the variation of the amplitude of the magnetization is smallest. The constant magnetization modulus $|M| = 1$ corresponds to the magnetization in the conical phase.

however, with an underlying sixfold symmetry. This behavior is strongly reminiscent of domain populations in superconducting flux line lattices (see, e.g., [46] and references therein) and provides strong empirical evidence against a multi-domain single-$\vec{k}$ state.

In conclusion, our studies of the magnetic properties across the B20 series of transition metal compounds MnSi, $Mn_{1-x}Fe_xSi$, $Mn_{1-x}Co_xSi$ and $Fe_{1-x}Co_xSi$, establish that the spin structure of the A-phase in all of these systems forms a skyrmion lattice for the values of x studied. This implies that the underlying mechanisms are sufficiently general to protect the formation of skyrmion lattices against disorder and regardless whether the electronic structure is that of a pure metal or a strongly disordered semiconductor.

Acknowledgments

We gratefully acknowledge discussions with E M Forgan, M Garst, A Vishnawath, M Vojta and K Everschor and the support of B Russ, A Regnat, T Merx and the team from FRM II.

References

[1] Ishikawa Y *et al* 1985 *Phys. Rev.* B **31** 5884
[2] Lonzarich G G and Taillefer L 1985 *J. Phys. C: Solid State Phys.* **18** 4339
[3] Moriya T 1985 *Spin Fluctuations in Itinerant Electron Magnetism* (*Solid-State Sciences* vol 56) (Berlin: Springer)
[4] Pfleiderer C, Böni P, Keller T, Rößler U K and Rosch A 2007 *Science* **316** 1871
[5] Miyake A, Villaume A, Haga Y, Knebel G, Salce B, Lapertot G and Flouquet J 2009 *J. Phys. Soc. Japan* **78** 044703 arXiv:0901.4435
[6] Ishikawa Y and Arai M 1984 *J. Phys. Soc. Japan* **53** 2726
[7] Janoschek M, Bernlochner F, Dunsiger S, Pfleiderer C, Böni P, Roessli B, Link P and Rosch A 2009 arXiv:0907.5576
[8] Thompson J D, Fisk Z and Lonzarich G G 1989 *Physica* B **161** 317
[9] Pfleiderer C, Friend R H, Lonzarich G G, Bernhoeft N R and Flouquet J 1993 *Int. J. Mod. Phys.* B **7** 887
[10] Pfleiderer C 2009 *Rev. Mod. Phys.* **81** 1551
[11] Pfleiderer C, McMullan G J, Julian S R and Lonzarich G G 1997 *Phys. Rev.* B **55** 8330
[12] Pfleiderer C, Julian S R and Lonzarich G G 2001 *Nature* **414** 427–30
[13] Pfleiderer C 2003 *Physica* B **328** 100–4
[14] Doiron-Leyraud N, Walker I R, Taillefer L, Steiner M J, Julian S R and Lonzarich G G 2003 *Nature* **425** 595–9
[15] Pfleiderer C 2007 *J. Low Temp. Phys.* **147** 231
[16] Bernhoeft N R 1996 Personal communication based on SANS studies
[17] Petrova A E, Krasnorussky V N, Lograsso T A and Stishov S M 2009 *Phys. Rev.* B **79** 100401
[18] Pfleiderer C, Reznik D, Pintschovius L, v Löhneysen H, Garst M and Rosch A 2004 *Nature* **427** 227–30
[19] Mühlbauer S, Binz B, Jonietz F, Pfleiderer C, Rosch A, Neubauer A, Georgii R and Böni P 2009 *Science* **323** 915
[20] Neubauer A, Pfleiderer C, Binz B, Rosch A, Ritz R, Niklowitz P G and Böni P 2009 *Phys. Rev. Lett.* **102** 186602
[21] Uemura Y J, Goko T, Gat-Malureanu I M, Carlo J P, Russo P L, Savici A T, Aczel A, MacDougall G J, Rodoriguez J, Luke G M, Dunsiger S R, McCollam A, Arai J, Pfleiderer C, Böni P, Yoshimura K, Baggio-Saitovitch E, Fontes M B, Larrea J, Sushko Y V and Sereni J 2007 *Nat. Phys.* **3** 34
[22] Binz B, Vishwanath A and Aji V 2006 *Phys. Rev. Lett.* **96** 207202
[23] Binz B and Vishwanath A 2006 *Phys. Rev.* B **74** 214408
[24] Rößler U K, Bogdanov A N and Pfleiderer C 2006 *Nature* **442** 797
[25] Tewari S, Belitz D and Kirkpatrick T R 2006 *Phys. Rev. Lett.* **96** 047207
[26] Fischer I, Shah N and Rosch A 2008 *Phys. Rev.* B **77** 024415
[27] Bogdanov A N and Yablonskii D A 1989 *Sov. Phys.—JETP* **68** 101–3
[28] Bogdanov A and Hubert A 1994 *J. Magn. Magn. Mater.* **138** 255–69
[29] Lebech B 1993 *Recent Advances in Magnetism of Transition Metal Compounds* (Singapore: World Scientific) p 167
[30] Lebech B, Harris P, Pedersen J S, Mortensen K, Gregory C, Bemhoeft N, Jermy M and Brown S 1995 *J. Magn. Magn. Mater.* **140–144** 119
[31] Grigoriev S V, Maleyev S V, Okorokov A I, Chetverikov Y O and Eckerlebe H 2006 *Phys. Rev.* B **73** 224440
[32] Birkelbach F 2009 Zulassungsarbeit Lehramt Technische Universität München
[33] Mühlbauer S 2005 *Diploma Thesis* Technische Universität München
[34] Guy C N 1978 *Solid State Commun.* **25** 169
[35] Beille J, Voiron J and Roth M 1983 *Solid State Commun.* **47** 399
[36] Grigoriev S V, Maleyev S V, Dyadkin V A, Menzel D, Schoenes J and Eckerlebe H 2007 *Phys. Rev.* B **76** 092407

[37] Grigoriev S V, Dyadkin V A, Moskvin E V, Lamago D, Wolf T, Eckerlebe H and Maleyev S V 2009 *Phys. Rev.* B **79** 144417
[38] Bauer A 2009 *Diploma Thesis* Technische Universität München
[39] Adams T 2009 *Diploma Thesis* Technische Universität München
[40] Münzer W, Neubauer A, Adams T, Mühlbauer S, Franz C, Jonietz F, Georgii R, Böni P, Pedersen B, Schmidt M, Rosch A and Pfleiderer C 2010 *Phys. Rev.* B **81** 041203
[41] Grigoriev S V, Chernyshov D, Dyadkin V A, Dmitriev V, Maleyev S V, Moskvin E V, Menzel D, Schoenes J and Eckerlebe H 2009 *Phys. Rev. Lett.* **102** 037204
[42] Grigoriev S V, Dyadkin V A, Menzel D, Schoenes J, Chetverikov Y O, Okorokov A I, Eckerlebe H and Maleyev S V 2007 *Phys. Rev.* B **76** 092407
[43] Takeda M, Endoh Y, Kakurai K, Onose Y, Suzuki J and Tokura Y 2009 *J. Phys. Soc. Japan* **78** 093704
[44] Adams T, Mühlbauer S, Neubauer A, Münzer W, Jonietz F, Georgii R, Pedersen B, Böni P, Rosch A and Pfleiderer C 2010 *J. Phys.: Conf. Ser.* **200** 032001
[45] Binz B and Vishwanath A 2008 *Physica* B **403** 1336–40
[46] Mühlbauer S, Pfleiderer C, Böni P, Laver M, Forgan E M, Fort D, Keiderling U and Behr G 2009 *Phys. Rev. Lett.* **102** 136408